Acta Crystallographica Section D
Biological Crystallography
ISSN 0907-4449

Structural basis for inhibition of *Escherichia coli* uridine phosphorylase by 5-substituted acyclouridines

Weiming Bu,[a] Ethan C. Settembre,[a] Mahmoud H. el Kouni[b] and Steven E. Ealick[a]*

[a]Department of Chemistry and Chemical Biology, Cornell University, Ithaca, NY 14853-1301, USA, and [b]Department of Pharmacology and Toxicology, Center for Aids Research, Comprehensive Cancer Center, University of Alabama at Birmingham, Birmingham, AL 35294, USA

Correspondence e-mail: see3@cornell.edu

Received 4 March 2005
Accepted 11 March 2005

PDB References:
UP–BAU–phosphate, 1u1c, r1u1csf; UP–PTAU–phosphate, 1u1d, r1u1dsf; UP–PSAU–phosphate, 1u1e, r1u1esf; UP–BBAU–phosphate, 1u1f, r1u1fsf; UP–BBBA, 1u1g, r1u1gsf.

Uridine phosphorylase (UP) catalyzes the reversible phosphorolysis of uridine to uracil and ribose 1-phosphate and is a key enzyme in the pyrimidine-salvage pathway. *Escherichia coli* UP is structurally homologous to *E. coli* purine nucleoside phosphorylase and other members of the type I family of nucleoside phosphorylases. The structures of 5-benzylacyclouridine, 5-phenylthioacyclouridine, 5-phenylselenenylacyclouridine, 5-*m*-benzyloxybenzyl acyclouridine and 5-*m*-benzyloxybenzyl barbituric acid acyclonucleoside bound to the active site of *E. coli* UP have been determined, with resolutions ranging from 1.95 to 2.3 Å. For all five complexes the acyclo sugar moiety binds to the active site in a conformation that mimics the ribose ring of the natural substrates. Surprisingly, the terminal hydroxyl group occupies the position of the nonessential 5′-hydroxyl substituent of the substrate rather than the 3′-hydroxyl group, which is normally required for catalytic activity. Until recently, inhibitors of UP were designed with limited structural knowledge of the active-site residues. These structures explain the basis of inhibition for this series of acyclouridine analogs and suggest possible additional avenues for future drug-design efforts. Furthermore, the studies can be extended to design inhibitors of human UP, for which no X-ray structure is available.

1. Introduction

Uridine phosphorylase (UP; EC 2.4.2.3) is a critical enzyme of pyrimidine-salvage pathways, where it catalyzes the reversible phosphorylation of both ribosides and 2′-deoxyribosides of uracil, as well as their analogs, to the respective nucleobases and (2′-deoxy)ribose 1-phosphate. Compared with UPs from other sources, *Escherichia coli* UP (EcUP) is more specific, acting almost exclusively on uridine and its analogs as substrates (Krenitsky *et al.*, 1964; Leer *et al.*, 1977; Vita *et al.*, 1986).

EcUP is active as a homohexamer with a total molecular weight of ∼165 kDa, with each monomer comprised of 253 amino acids. The structure of this enzyme has been determined previously in the unliganded form (Burling *et al.*, 2003; Morgunova *et al.*, 1995) and in substrate- and product-bound forms (Caradoc-Davies *et al.*, 2004). Structural evidence confirmed the prediction from sequence analysis that UP is a member of the nucleoside phosphorylase I (NP-I) family of proteins and hence shares a common fold with trimeric and hexameric purine nucleoside phosphorylases (PNP), methylthioadenosine phosphorylases (MTAP), *S*-adenosylhomocysteine/methylthioadenosine nucleosidase and AMP nucleosidase (Pugmire & Ealick, 2002). As a member of this family, EcUP most likely shares a similar mechanism for the

phosphorolysis reaction, which involves the formation of a high-energy ribosyloxocarbenium ion intermediate.

Several acylouridine analogs have been synthesized (Drabikowska, Lissowska, Draminski *et al.*, 1987; Drabikowska, Lissowska, Veres *et al.*, 1987; el Kouni *et al.*, 2000; Goudgaon *et al.*, 1993; Levesque *et al.*, 1993; Naguib *et al.*, 1987, 1993; Niedzwicki *et al.*, 1981, 1982; Orr *et al.*, 1997) as potent and specific inhibitors of UP from different sources (Ashour *et al.*, 2000; Drabikowska, Lissowska, Draminski *et al.*, 1987; Drabikowska, Lissowska, Veres *et al.*, 1987; el Kouni *et al.*, 1988, 1996, 2000; Goudgaon *et al.*, 1993; Levesque *et al.*, 1993; Naguib *et al.*, 1987, 1993; Niedzwicki *et al.*, 1981, 1982, 1983; Orr *et al.*, 1997), including EcUP (Drabikowska, Lissowska, Draminski *et al.*, 1987; Drabikowska, Lissowska, Veres *et al.*, 1987; Park *et al.*, 1986). These inhibitors were used to prevent the UP-catalyzed degradation of several chemotherapeutic pyrimidine nucleosides (Ashour *et al.*, 2000). However, the binding mechanism of these inhibitors to UP has not been elucidated.

In the present study, we investigated the binding mode of some of these acyclouridines to EcUP (Fig. 1). The inhibitors studied contain an acycloribosyl moiety and a pyrimidine nucleobase with a hydrophobic 5-substituent and can be divided into two classes. Class 1 inhibitors include 5-benzylacyclouridine (BAU; Naguib *et al.*, 1987; Niedzwicki *et al.*, 1982), 5-phenylthioacyclouridine (PTAU; el Kouni *et al.*, 2000) and 5-phenylselenenylacyclouridine (PSAU; Ashour *et al.*, 2000; Goudgaon *et al.*, 1993). Class 2 inhibitors include 5-*m*-benzyloxybenzyl acylouridine (BBAU; Naguib *et al.*, 1987; Niedzwicki *et al.*, 1982) and 5-*m*-benzyloxybenzyl barbituric acid acyclonucleoside (BBBA; Levesque *et al.*, 1993; Naguib *et al.*, 1993). BBAU is similar to BAU but has an additional benzyloxy moiety at the *meta* position of the 5-benzyl moiety attached to the uracil base. BBBA is similar to BBAU but has an additional O atom at the 6-position of the uracil ring. We determined the structures of EcUP complexed with each of these five inhibitors to aid in defining important active-site contacts. The structures define the basis for inhibition of EcUP by this family of acyclouridine analogs. Comparison of the amino-acid sequences of human UP (hUP) and EcUP suggests that the structural results for the *E. coli* enzyme can be extrapolated to the human enzyme. The structural data together with recent developments in the discovery of UP inhibitors suggest possible improvements for inhibitor design.

2. Experimental procedures

2.1. Compounds

BAU and BBAU (Naguib *et al.*, 1987; Niedzwicki *et al.*, 1982), PTAU (el Kouni *et al.*, 2000), PSAU (Goudgaon *et al.*, 1993) and BBBA (Levesque *et al.*, 1993; Naguib *et al.*, 1993) were synthesized as described previously.

2.2. Protein purification

The EcUP gene was cloned into the overexpression plasmid pET16b and transformed into *E. coli* strain BL21 (DE3) (Novagen). The cells were grown in 2 l Luria–Bertani media supplemented with 200 µg ml^{-1} ampicillin. They were grown at 310 K until they reached an OD_{600} of approximately 0.6, at which point they were induced with 1 m*M* isopropyl-β-D-thiogalactoside and allowed to grow for an additional 6 h at 310 K. Cells were harvested by centrifugation.

The cells were resuspended in 100 ml binding buffer (10 m*M* Tris–HCl, 5 m*M* imidazole, 450 m*M* NaCl, 1 m*M* β-mercaptoethanol pH 8.0) and lysed by two passages through a French press. Cell debris was removed by centrifugation and the cleared lysate was loaded onto a 20 ml bed volume of Talon resin (Clontech) at a flow rate of 1 ml min^{-1} using an AKTA FPLC (American Biosciences). After the crude extract had been loaded, the column was washed with 100 ml binding buffer at a flow rate of 5 ml min^{-1}. EcUP was eluted from the column with elution buffer (10 m*M* Tris–HCl, 200 m*M* imidazole, 250 m*M* NaCl, 1 m*M* β-mercaptoethanol pH 8.0). The eluted protein was buffer-exchanged into final storage

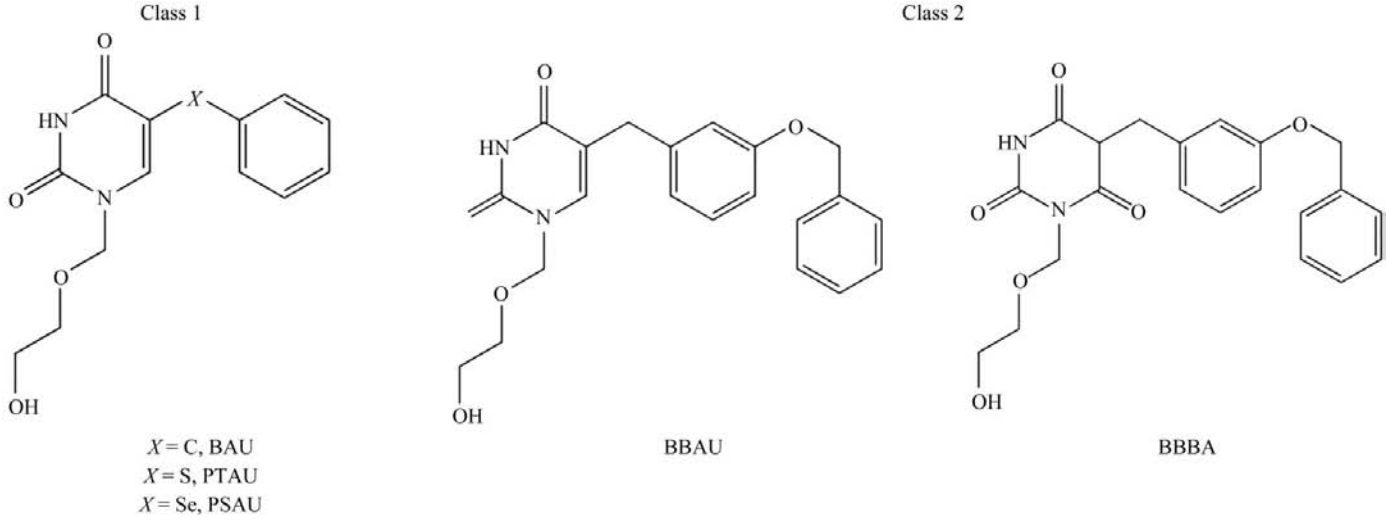

Figure 1
Inhibitors used in the current study.

buffer (100 m*M* NaCl, 1 m*M* DTT and 10 m*M* Tris–HCl pH 8.0) and concentrated to 10 mg ml^{-1} using a 10 kDa molecular-weight cutoff concentrator (Millipore).

At this point, the polyhistidine tag was cleaved with an overnight digest at 277 K using biotinylated thrombin (1 U per milligram of protein) in 1× thrombin cleavage buffer (Novagen). The cleaved protein was run over both a streptavidin resin and an Ni–NTA column to remove the thrombin, the polyhistidine tag and any uncut protein. The remaining protein was dialyzed back into the final buffer at 277 K, concentrated to 10 mg ml^{-1} and stored at 193 K. The purity of EcUP was determined by Coomassie-stained SDS–PAGE analysis and found to be greater than 99% (data not shown).

2.3. Crystallization of the EcUP complexes

Concentrated enzyme (10 mg ml^{-1}) was incubated separately with 1 m*M* each of the five inhibitors (BAU, PTAU, PSAU, BBAU or BBBA) and 10 m*M* ammonium phosphate for 1 h prior to crystallization. The protein crystallized under conditions very similar to those used by Burling *et al.* (2003). Crystals were grown by the hanging-drop method in 5–7% PEG 4K, 0.1 *M* MES pH 6.2–6.3 and 25% glycerol at 295 K. Crystals grew over 2 d to maximum dimensions of ~300 × 300 × 200 µm. The crystal trays were transferred to 277 K and allowed to equilibrate at this temperature before harvesting. The crystals were frozen while at 277 K with a quick dunk into liquid nitrogen and were stored until use.

Preliminary X-ray analysis showed that all of the crystals belong to space group $P2_12_12_1$ and have similar unit-cell parameters of approximately a = 91.2, b = 125.8, c = 140.9 Å, even though the unliganded protein crystallized in space group $R3$ under the same conditions. The EcUP complex crystals contain one complete hexamer per asymmetric unit, corresponding to a solvent content of 47%. All the EcUP complex crystals diffracted to about 2.0 Å resolution.

2.4. Data collection and processing

Single-wavelength data (λ = 0.979 Å) for the BBBA, PTAU, PSAU and BAU complexes were measured at beamline 8BM at the Advanced Photon Source (APS) using a Quantum 315 detector (Area Detector Systems Corporation). Data for the BBAU complex were measured with a Rigaku RU-200 rotating-anode generator using Cu $K\alpha$ radiation and a Rigaku R-AXIS IV^{++} image-plate detector with an Oxford Cryostream System cooling device. The data were processed using *HKL*2000 (Otwinowski & Minor, 1997). Data-collection and data-processing statistics are summarized in Table 1.

2.5. Structure determination, model building and refinement

The EcUP complex structures were determined by molecular replacement using the program *CNS* (Brünger *et al.*, 1998), with all the protein atoms of the previously reported native UP monomer structure (PDB code 1lx7) as the search model (Burling *et al.*, 2003). The refinement procedure involved successive rounds of rigid-body refinement, simulated-annealing refinement, temperature-factor refinement and model rebuilding. Difference maps were examined to determine the active-site contents and to identify alternate conformations of side chains. Side chains and regions showing poorly defined peptide backbone electron density were then manually adjusted using the program *O* (Jones *et al.*, 1991). In particular, the loop containing residues 225–232 was weakly visible in the density for all five structures and sometimes appeared to have multiple conformations; however, the loop

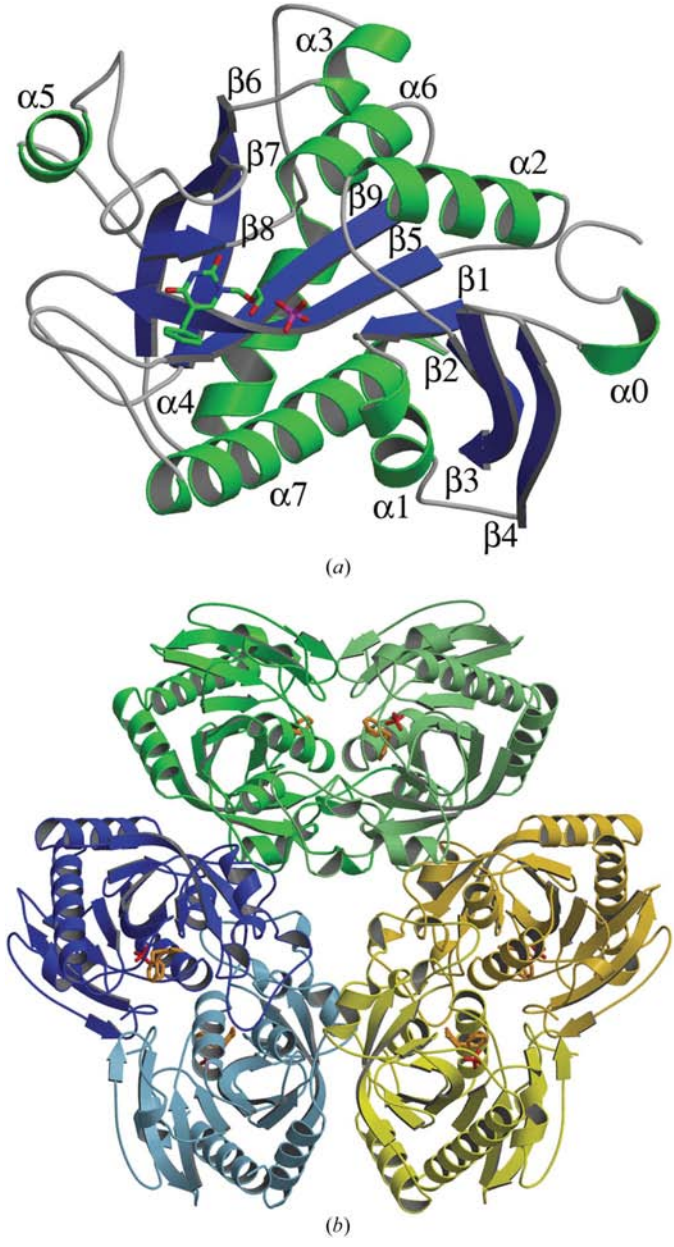

Figure 2
Structure of UP shown in ribbon representation. (*a*) UP monomer with β-strands in blue and α-helices in green. BAU and phosphate are shown in stick representation bound at the active site. C atoms are colored green, N atoms blue, O atoms red and P atoms pink. (*b*) UP hexamer shown in ribbon representation with BAU (orange) and phosphate (red) shown bound at the active sites. Dimers with greater buried surface area are shown in similar colors. This figure was prepared with *MOLSCRIPT* (Kraulis, 1991) and *RASTER3D* (Merritt & Bacon, 1997).

Table 1
Data-collection statistics.

Values in parentheses are for the last resolution shell.

	UP–BAU–PO_4	UP–PTAU–PO_4	UP–PSAU–PO_4	UP–BBAU–PO_4	UP–BBBA
Resolution (Å)	2.2	2.0	2.0	2.3	1.95
Space group	$P2_12_1\,2_1$	$P2_12_1\,2_1$	$P2_12_1\,2_1$	$P2_12_1\,2_1$	$P2_12_1\,2_1$
Unit-cell parameters (Å)					
a	91.4	91.2	91.1	91.6	92.7
b	126.0	125.8	125.7	125.8	127.1
c	141.3	140.9	140.9	141.1	143.4
No. of reflections	542903	801290	653898	430936	704450
No. of unique reflections	83127	109591	108334	72892	118727
Redundancy	6.5 (6.0)	7.3 (6.4)	6.0 (4.4)	5.9 (5.9)	5.9 (3.6)
Completeness	99.9 (99.9)	99.9 (99.9)	99.1 (94.6)	99.8 (100)	94.9 (71.1)
R_{sym}† (%)	5.4 (33.1)	4.9 (34.5)	6.4 (34.4)	6.9 (36)	5.3 (32.5)
$I/\sigma(I)$	30.0 (6.05)	33.3 (5.14)	24.8 (3.36)	26.1 (4.87)	24.5 (3.31)

† $R_{sym} = \sum\sum_i |I_i - \langle I\rangle| / \sum\langle I\rangle$, where $\langle I\rangle$ is the mean intensity of the N reflections with intensities I_i and common indices *hkl*.

Table 2
Refinement statistics.

	UP–BAU–PO_4	UP–PTAU–PO_4	UP–PSAU–PO_4	UP–BBAU–PO_4	UP–BBBA
Resolution (Å)	40–2.2	50–2.0	50–2.0	50–2.3	50–1.95
No. of non-H atoms	11925	11932	11953	11915	12025
No. of protein atoms	11211	11273	11273	11178	11156
No. of water atoms	561	506	527	536	692
No. of ligand atoms	150	150	150	198	174
No. of K atoms	3	3	3	3	3
R factor† (%)	21.6	20.9	21.1	19.9	20.0
R_{free}‡ (%)	24.9	22.6	23.5	22.8	22.1
Ramachandran plot					
Most favored region (%)	90.5	90.7	90.8	90.6	90.4
Additionally allowed region (%)	9.0	8.7	8.4	8.8	9.1
Generously allowed region (%)	0.3	0.5	0.7	0.5	0.4
Disallowed region (%)	0.2	0.1	0.1	0.1	0.1
R.m.s. deviations from ideal					
Bonds (Å)	0.005	0.005	0.005	0.005	0.006
Angles (°)	0.89	0.90	0.89	0.89	0.90
Average *B* factors (Å^2)					
Protein	21.8	16.8	11.5	14.4	14.9
Water	37.4	38.8	37.4	39.0	37.6
Ligand	34.8	38.4	35.1	42.5	37.6
Potassium	61.9	65.1	61.8	65.0	58.5

† R factor $= \sum_{hkl} ||F_{obs}| - k|F_{calc}|| / \sum_{hkl} |F_{obs}|$, where F_{obs} and F_{calc} are the observed and calculated structure factors, respectively. ‡ For R_{free}, the sum is extended over a subset of reflections excluded from all stages of refinement. The test set contained 7% of the total reflections for the BBAU and BBBA complexes and 10% of the remaining complexes.

was always built into the strongest density. In a few monomers there was no clear density for the loop and these residues were excluded from the model. NCS restraints were applied to residues 50–223 throughout model building to improve density in weaker regions and in general the restraint was relaxed during successive rounds of refinement. Ligands were generated using *PRODRG*2 (van Aalten *et al.*, 1996) and positioned into clear $F_o - F_c$ map density after refinement of the full-atom protein model had converged. Phosphate ions, water molecules and potential potassium ions were then added and refined in *CNS*. The final models from *CNS* were transferred to *REFMAC*5 (Murshudov *et al.*, 1999) and refined for a few more cycles using TLS parameters and loose NCS restraints.

Each of the six crystallographically independent active sites was occupied by a single inhibitor molecule and a phosphate ion, except for the UP–BBBA complex, which only contained a molecule of BBBA at every active site. Furthermore, three potassium ions were found at the interfaces of the UP dimers as previously observed (Caradoc-Davies *et al.*, 2004). Although potassium was not explicitly added during either the crystallization or the purification, it may have copurified or been present as a contaminant in the crystallization solutions. Although the potassium ion *B* factors are high, suggesting partial occupancy, the assignment of potassium is suported by the observed ligand bond distances. The structures refined to final *R* factors ranging from 20.3 to 21.7%, with all structures having >89% of backbone torsion angles in the most favored region of the Ramachandran plot. The models were examined using *PROCHECK* (Laskowski *et al.*, 1993) and no abnormalities were detected. The final refinement statistics are summarized in Table 2.

3. Results

3.1. Overall structure of the EcUP complexes

The overall fold is similar to the other members of the NP-I family of proteins (Fig. 2*a*; Pugmire & Ealick, 2002). As such, a monomer consists of one large eight-stranded mixed β-sheet flanked on one side by four α-helices and on the other side by three α-helices and a shorter five-stranded mixed β-sheet. There is an additional 3_{10}-helix found prior to the first β-strand that is not generally present in the other NP-I family members.

The EcUP homohexamer displays D_3 symmetry (Burling *et al.*, 2003; Caradoc-Davies *et al.*, 2004; Morgunova *et al.*, 1995). The enzyme is disc-shaped with a diameter of ~100 Å and a thickness of 40 Å. A long channel (~28 Å) with an ~6 Å wide opening at each end runs through the center of the hexamer. The hexameric quaternary structure of EcUP can be described as a 'trimer of dimers' in which each dimer contains two complete active sites. The active sites are located at the dimer interface and each of the monomers contributes residues to each of the active sites (Caradoc-Davies *et al.*, 2004). In Fig. 2(*b*), the monomers that form these tight dimers are indicated in similar colors. This arrangement is nearly identical to that found in *E. coli* PNP (EcPNP; Bennett *et al.*, 2003), *Sulfolobus sulfataricus* methylthioadenosine phosphorylase (Appleby *et al.*, 2001) and the core of AMP nucleosidase (Zhang *et al.*, 2004).

3.2. EcUP active site

The structure of EcUP has previously been determined (Burling *et al.*, 2003; Morgunova *et al.*, 1995) and the residues involved in substrate binding and catalysis have previously been identified (Caradoc-Davies *et al.*, 2004). The five UP–inhibitor complexes reported here further define the active site and demonstrate the structural basis for UP inhibition by acyclouridine analogs (Fig. 3). The active site is located at the interface of two adjacent monomers and contains a cluster of highly conserved amino-acid residues. Each active site contains important residues donated from the closely related neighboring monomer. The active site can be divided into three parts: the pyrimidine-binding site, the ribose-binding site and the phosphate-binding site (Fig. 4).

In the pyrimidine-binding site, the O4 atom of the uracil base forms a hydrogen bond with both Arg168 and a water molecule that in turn hydrogen bonds to Arg223. In addition, the O2 and N3 atoms of uracil form hydrogen bonds with Gln166. In the BBBA–UP complex, the O6 of the uracil base makes an additional hydrogen bond to Thr94 (2.9 Å). The base itself has herringbone stacking interactions with Phe162. Near the 5-position of the uracil base, there is a conserved hydrophobic pocket formed mainly by Ile220 and Val221. Upon inhibitor binding, an active-site loop including residues Ile228 and Pro229 also closes over the hydrophobic pocket to seal the active site.

In both class 1 and class 2 inhibitors, there is a large 5-substitutent on the pyrimidine base that points towards the solvent and is enclosed in this hydrophobic pocket. Phe162 from one monomer and Phe7 from the neighboring monomer provide additional hydrophobic interactions with the 5-substituent. A series of base-stacking interactions is observed that involve the uracil ring, the phenyl ring at the five position, Phe7, Phe162 and Tyr163. Furthermore, the benzyloxy moiety of class 2 inhibitors makes additional hydrophobic interactions with Met234, whose side chain rotates 180° from its original position upon inhibitor binding.

The ribose-binding site can accommodate either a ribosyl or 2′-deoxyribosyl moiety. In all the inhibitor structures, the acycloribose tail binds in a similar conformation with only minor differences in the positions of the C3′ and C4′ atoms.

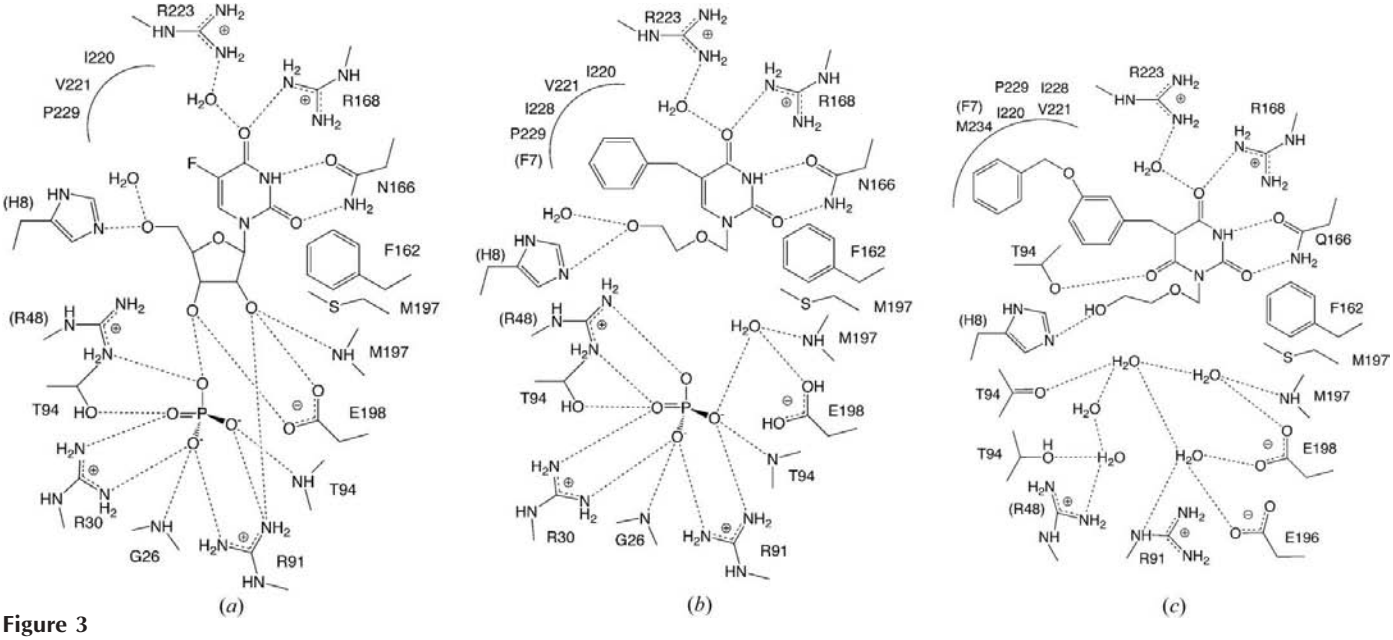

Figure 3
Schematic representation of the UP active site with bound (*a*) 5-fluorouridine and phosphate, (*b*) BAU and phosphate or (*c*) BBBA. Hydrogen bonds are shown in dashed lines. The active-site hydrophobic pocket is indicated by a solid line flanked by the participating residues.

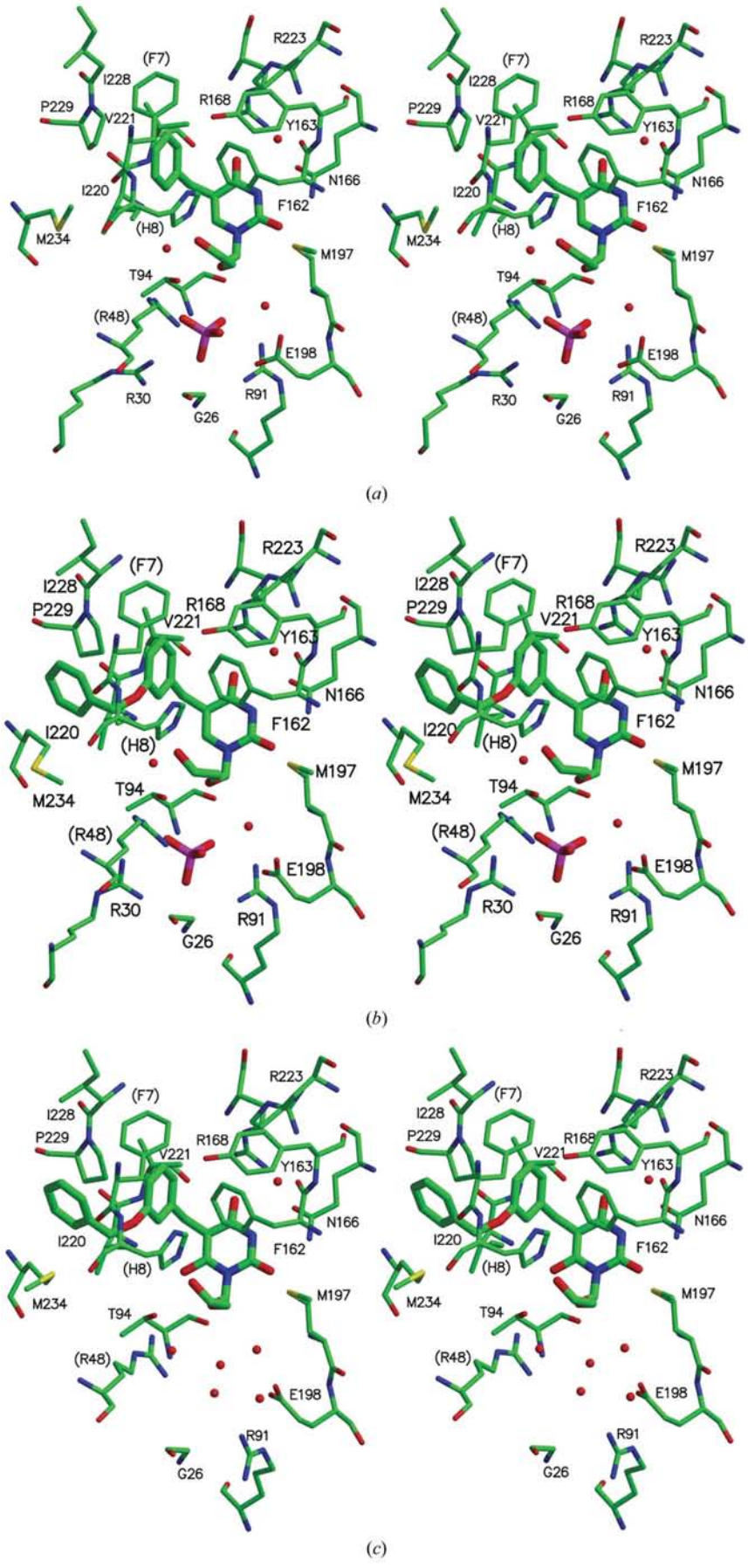

The terminal hydroxyl O5′ atom hydrogen bonds to $N^{\epsilon 2}$ of the absolutely conserved active-site residue His8 with a distance of ∼2.8 Å. In all inhibitor structures except BBBA, the terminal hydroxyl has an additional hydrogen bond to an active-site water molecule. Structures of EcUP bound with substrates and products indicated that the 5′-hydroxyl of the ribose moiety has hydrogen-bonding interactions with both His8 and the active-site water (Caradoc-Davies *et al.*, 2004).

The phosphate-binding site is nearer to the surface than the nucleoside-binding site. The binding of the phosphate ion involves side-chain interactions from Arg30, Arg91 and Thr94 from one subunit, and Arg48 from the neighboring subunit. There are also two important amide backbone hydrogen bonds, one from Thr94 and the other from Gly26. Sequence alignment with all known UPs indicates that all of the residues involved in the phosphate-binding site are absolutely conserved except Arg48, which can also be a lysine. In the UP–BBBA structure, no phosphate is bound and the side chain of Arg30 is not visible.

4. Discussion

4.1. Effect of the 5-substituent on inhibitor binding

Pyrimidine-base binding in the active site of EcUP is accompanied by a concerted closing motion of the active site (Caradoc-Davies *et al.*, 2004). A similar large motion is seen when comparing the unbound form of EcPNP with the bound form of EcPNP (Koellner *et al.*, 2002). The 'induced-fit' movement in EcUP involves an active-site loop containing residues 225–230 that acts as a lid over the pyrimidine-binding site upon ligand binding. In the entirely closed conformation, as observed with 5-fluorouridine (FUrd) bound (Caradoc-Davies *et al.*, 2004), Glu227 hydrogen bonds to the backbone N atom of Tyr169. Additionally,

Figure 4
Stereoview of three UP active sites shown with important residues drawn in stick representation. Waters are shown as red circles. C atoms are colored green, N atoms blue, O atoms red, S atoms yellow and P atoms pink. (*a*) BAU is shown bound with phosphate. (*b*) BBAU is shown bound with phosphate. (*c*) BBBA is shown alone. This figure was prepared with *MOLSCRIPT* (Kraulis, 1991) and *RASTER3D* (Merritt & Bacon, 1997).

Pro229 and Ile228 cover a hydrophobic pocket involving residues Ile220, Val221 and Phe7 as well as the C5 position of the uracil ring.

Inhibitor binding results in two major differences when compared with the substrate bound form of the enzyme (Fig. 5) (Caradoc-Davies *et al.*, 2004). Firstly, in both classes of inhibitors the first phenyl ring displaces Phe7, which was originally involved in covering the hydrophobic pocket on the side of the pyrimidine-binding pocket. The Phe7 side chain rotates ∼90° from its original position towards the solvent. In this new position, Phe7 continues to cover the active site, but now makes additional herringbone stacking interactions with the first phenyl ring attached to the base. Secondly, the loop region from residues 225–230 that has been shown to close entirely over the active site in the substrate complex (Caradoc-Davies *et al.*, 2004) remains partially open (∼2.5 Å) compared with the closed conformation. However, in the inhibitor complexes reported here the loop region is partially disordered and apparently takes on multiple conformations. Part of the first phenyl ring is solvent-exposed and Pro229 and Ile228 are involved in hydrophobic interactions with the phenyl ring. In substrate-bound structures, Glu227 has been shown to help stabilize the closed conformation of this loop by making hydrogen bonds to the backbone amides of Tyr169 and Asp170. When an inhibitor is bound, Glu227 does not form any hydrogen-bonding interactions with any other residue.

The class 2 inhibitors, which have an additional benzyloxy group, show two

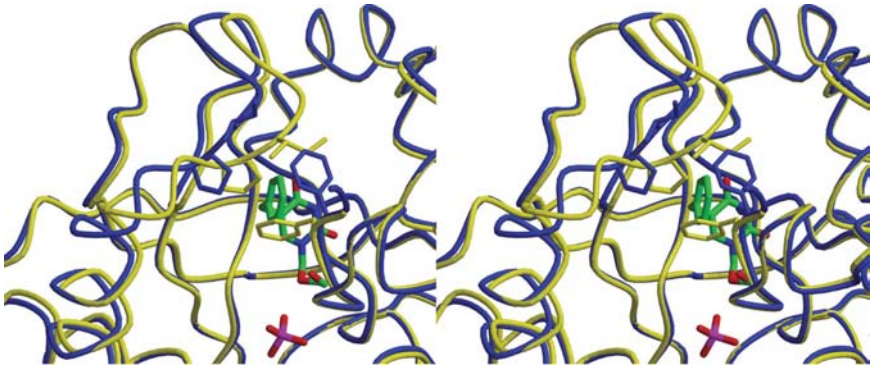

Figure 5
Comparison of UP active site when BAU is bound (yellow) or 5-fluorouridine is bound (blue). Phe7, Ile228 and Pro229 are shown in stick representation. BAU and phosphate are shown bound at the active site. C atoms are colored green, N atoms blue, O atoms red and P atoms pink. This figure was prepared with *MOLSCRIPT* (Kraulis, 1991) and *RASTER3D* (Merritt & Bacon, 1997).

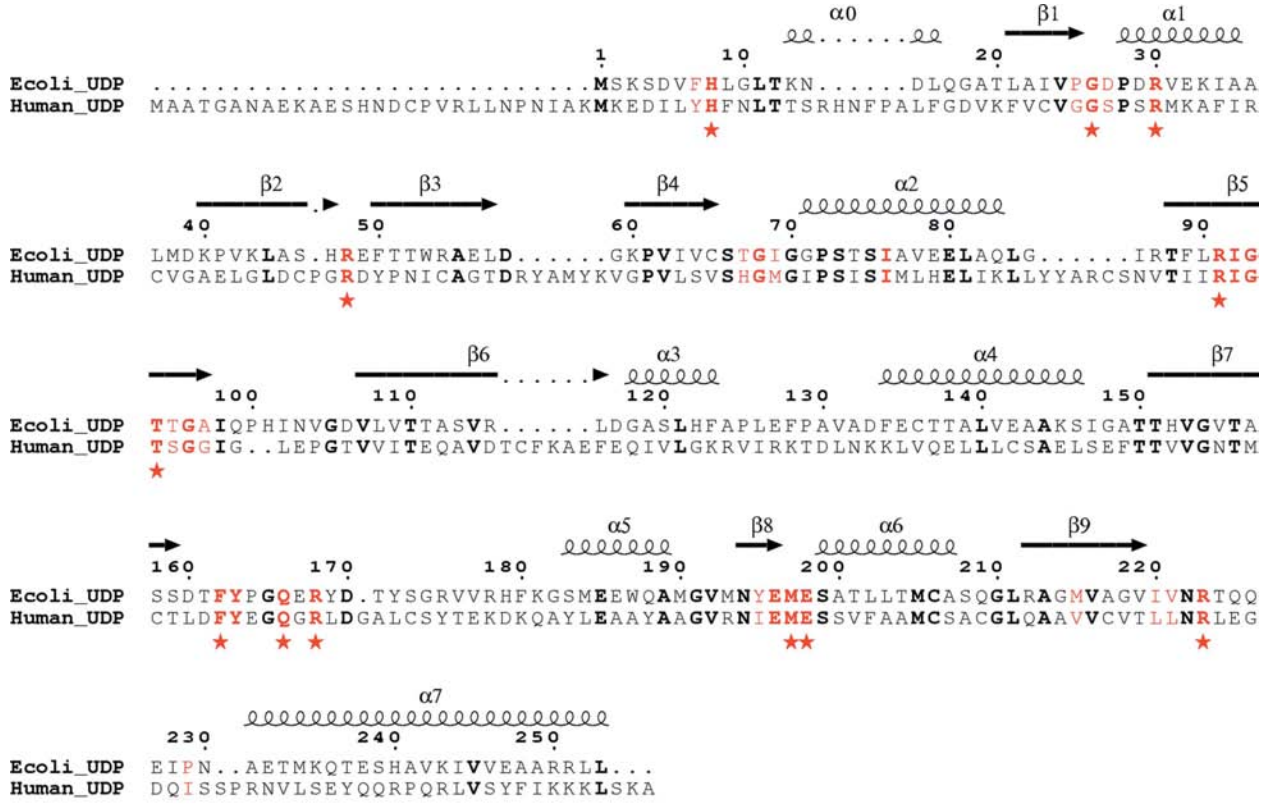

Figure 6
Sequence alignment of *E. coli* UP with human UP. The alignment is overlaid with the known tertiary structure of *E. coli* UP with structural elements labeled α for α-helices and β for β-strands. Residues found in the active site are colored red and those that have hydrogen-bonding interactions are starred. Residues that are identical are in bold. This figure was prepared with *ESPRIPT* (Gouet *et al.*, 1999).

Table 3
Published inhibition constants (K_i) of UP inhibitors for *E. coli* and human uridine phosphorylases.

N/D, not determined.

	K_i† (n*M*)	
Inhibitor	*E. coli*	Human
BAU	4300 ± 400	1190 ± 200
PTAU	N/D	353 ± 76
PSAU	N/D	340 ± 19
BBAU	680 ± 30	220 ± 29
BBBA	N/D	1.1 ± 0.2

† Values are means ± standard error of estimation from at least three determinations measured at 20 m*M* inorganic phosphate.

additional differences. Firstly, Ile228 and Pro229 move ∼1 Å farther away from the active site to accommodate the second benzyloxy moiety. One face of the second benzyloxy moiety is entirely exposed to the solvent, while the other stacks with Pro229. Secondly, the side chain of Met234 rotates ∼180° away from the active site and forms hydrophobic interactions with the second benzyloxy moiety.

4.2. Comparison of acycloribose binding with ribose binding

Acycloribose binding shows several similarities to the ribose binding in the structure of EcUP with FUrd and phosphate (Caradoc-Davies *et al.*, 2004). The acycloribose moiety of the inhibitors hydrogen bonds to His8 in a similar manner as O5′ of FUrd. C1′, O2′, C3′, C4′ and O5′ of the acycloribose moiety mimic the C1′, O4′, C4′, C5′ and O5′ positions of the ribose moiety of nucleosides, respectively. The inhibitor structures show that the positions for the C1′, O2′ and O5′ of the acycloribose moiety are in nearly identical positions in the inhibitor structures; however, the positions of the C3′ and C4′ atoms appear to be more variable. Unexpectedly, a strongly bound water at the EcUP active site binds in similar position to the O2′ of the ribosyl moiety of FUrd and forms an ∼2.6 Å hydrogen bond to Glu198. In addition, this active-site water forms an ∼2.8 Å hydrogen bond to an O atom of the bound phosphate in those inhibitor complexes that contain a phosphate. In the case of the BBBA–EcUP complex, this water molecule hydrogen bonds to another active-site water molecule and the backbone N atom of Met197.

The ribosyl or 2′-deoxyribosyl moiety of the nucleosides makes multiple hydrogen bonds to both the protein and the bound active-site phosphate (Appleby *et al.*, 1999, 2001; Caradoc-Davies *et al.*, 2004; Mao *et al.*, 1997, 1998). In contrast, the acycloribosyl moiety forms only two hydrogen-bonding interactions: one with His8 and another with an active-site water molecule, suggesting that the acycloribosyl moiety is much less constrained than the substrate ribosyl group.

4.3. Relationship of EcUP to hUP

Sequence alignment between EcUP and hUP reveals a 21% identity and 35% similarity (Fig. 6); however, almost all the active-site residues are absolutely conserved. This includes residues that bind to the nucleoside (His8, Met197, Glu198, Phe162, Gln166, Arg168 and Arg223) and those that bind the phosphate (Gly26, Arg30, Arg91 and Thr94). Only Arg48 in the phosphate-binding pocket is a different residue (lysine) in hUP. Eight additional active-site residues are conserved and eight more have a conserved charge. The high degree of conservation of active-site residues suggests that these two proteins will have similar inhibition profiles.

Furthermore, EcUP and hUP are likely to have similar quaternary structures. Support for a hexameric hUP structure comes from analysis of the secondary-structural alignments of EcUP and EcPNP. Previous multiple sequence alignments of UPs identified regions of conservation not only in the active-site residues but also in residues at the dimer interface (Pugmire & Ealick, 2002). In particular, Phe7, His8 and Arg48 are donated to the active site of one monomer by the neighboring monomer. In hUP, the active-site histidine that forms a hydrogen bond with the 5′-hydroxyl group of the nucleoside is conserved, while Phe7 is replaced by tyrosine and Arg48 is replaced by lysine. Phe7 covers the active site upon nucleoside binding and Arg48 binds the active-site phosphate. The tyrosine and lysine in hUP could fulfill these functional roles. This supports the formation of a tight dimer characteristic of the hexameric form of NP-I family members.

Currently, the only three known mammalian NP-I family members, human MTAP, bovine PNP and human PNP, are trimers; however, the prokaryotic proteins can be either trimers or hexamers. UP has the unique distinction in the NP-I family that it is specific for pyrimidine nucleosides. The other pyrimidine nucleoside phosphorylases, thymidine phosphorylase (Pugmire *et al.*, 1998; Walter *et al.*, 1990) and pyrimidine nucleoside phosphorylase (Pugmire & Ealick, 1998), are dimers and members of the NP-II family of proteins. Sequence comparisons suggest that mammalian UPs are unlikely to have the trimeric structures observed for mammalian PNPs (Ealick *et al.*, 1990; Mao *et al.*, 1998) and MTAPs (Appleby *et al.*, 1999).

Previous experiments measured the inhibition of EcUP (Levesque *et al.*, 1993; Niedzwicki *et al.*, 1982; Park *et al.*, 1986) and hUP (Drabikowska, Lissowska, Draminski *et al.*, 1987; Drabikowska, Lissowska, Veres *et al.*, 1987; el Kouni *et al.*, 2000; Orr *et al.*, 1997) by BAU and BBAU (Table 3). These experiments showed that BBAU inhibited both enzymes more strongly than BAU. Additional experiments showed that PTAU (Drabikowska, Lissowska, Draminski *et al.*, 1987; Drabikowska, Lissowska, Veres *et al.*, 1987) and PSAU (Ashour *et al.*, 2000) inhibited hUP more strongly than BAU and that BBBA (Orr *et al.*, 1997) was a more potent inhibitor than PTAU or PSAU. These observations for hUP are consistent with the corresponding structures of the EcUP inhibitor complexes.

4.4. Factors affecting inhibitor binding affinity

Analysis of the inhibitor complexes suggests possible reasons for increased binding based on inhibitor–protein interactions. Class 1 inhibitors have increased interactions in the hydrophobic binding area covering the pyrimidine-binding

site compared with the substrate complexes. However, there are no obvious different structural features that account for greater inhibition by PTAU and PSAU compared with BAU. In addition, it is clear that the hydrogen bond between His8 and the acycloribosyl moiety would account for improved binding compared with the benzyluracil base alone (Naguib *et al.*, 1987).

Class 2 inhibitors have an additional benzyloxy group and therefore additional hydrophobic interactions that may account for the increased level of inhibition compared with class 1 inhibitors. The benzyloxy moiety stacks with Pro229 when the active site is in the closed position. This additional binding interaction may further stabilize the closed form of the active site. BBBA has a higher level of inhibition than BBAU for hUP (Orr *et al.*, 1997). The hydrogen bond between the O6 atom of the barbituric acid base and the side chain of Thr94 may account for the higher level of inhibition. This interaction may also account for the absence of phosphate in the structure of the EcUP–BBBA complex.

4.5. Structural basis for inhibition

The catalytic mechanism proposed for UP and other NP-I family members involves the binding of the nucleoside in a strained C4′-*endo* conformation. This high-energy conformation puts strain on the N—C1′ bond between the pyrimidine base and the ribose. As the glycosidic bond begins to break, the pyrimidine base accepts the building negative charge and is stabilized by the donation of a proton to the O4 position of the base by either Arg168 or by a water hydrogen bonded to both O4 and Arg223. Recent mutagenesis studies have indicated that Arg168 is absolutely required for activity and is the probable proton donor (unpublished results). The resulting oxocarbenium ion collapses with phosphate to form the final product, ribose 1-phosphate.

The main effect of the inhibitors reported here results from their ability to bind strongly to the protein and their inability to form the required oxocarbenium ion and cleave. The acycloribose moiety mimics the C1′, O4′, C4′, C5′ and O5′ atoms of the substrate ribose. The structures show that the interactions with the terminal hydroxyl group of the acycloribose moiety are conserved in substrate–protein interactions; however, there are no other hydrogen-bonding interactions between the acycloribose moiety and the protein. This acyclic nature of the N1 substituent, the lack of protein interactions with the acycloribose moiety and the lack of a hydrogen bond to orient the phosphate group help explain why the acyclic analogs are catalytically inactive.

4.6. Potential inhibitor design

Previously published studies indicate that increasing substitution on the acycloribose moiety may result in more potent inhibitors (Cha, 1989). In particular, the addition of an aminomethyl or hydroxymethyl group onto the C3′ position of the acycloribose increases the potency of inhibition (Drabikowska, Lissowska, Draminski *et al.*, 1987; Drabikowska, Lissowska, Veres *et al.*, 1987). These additional groups may mimic the O3′ position of ribose and generate additional protein interactions. Based on the structures, a hydrogen bond between the O3′-substituent and the side of Glu198 or the phosphate is likely.

The structures of BBAU and BBBA indicate that the partially conserved Glu223 (glutamine in humans) can no longer bind the backbone N atom of Tyr169, which presumably aids in stabilizing the closed conformation of the active-site loop. Therefore, a positively charged moiety in a *meta* position of the final benzyloxy moiety of BBAU or BBBA may act as a hydrogen-bonding partner for this residue. This additional hydrogen bond should further stabilize the partially closed conformation of the active-site loop and increase the level of inhibition.

Finally, recent advances in 'transition-state' inhibitor design (immucillins) have dramatically improved the inhibition of other NP-I family members (Basso *et al.*, 2001; Kicska *et al.*, 2001; Lewandowicz *et al.*, 2003; Schramm, 2002, 2003; Shi *et al.*, 2001, 2004; Singh *et al.*, 2004). These inhibitors contain a noncleavable glycosidic bond and an N atom at the ribose 4′-position to mimic the charge of the ribosyl oxocarbenium ion intermediate. Transition-state analog inhibitors of human PNP and human MTAP have inhibition constants of 7 p*M* (Evans *et al.*, 2003) and 166 p*M* (Evans *et al.*, 2004), respectively. Given the similarity of the UP and PNP active sites and the expectation of similar catalytic mechanisms, it is likely that analogous transition-state analogs will be potent inhibitors of UP. Based on the structure–activity relationships derived from the studies reported here, further potency and specificity may be achieved by adding bulky substituents at the 5-position of the pyrimidine base.

We thank the Northeastern Collaborative Access Team at the Advanced Photon Source for provision of beam time. This work was supported by National Cooperative Drug Discovery Grant CA-67763 from the National Institutes of Health and by NIH grant RR-15301. SEE is indebted to the W. M. Keck Foundation and the Lucille P. Markey Charitable Trust.

References

Aalten, D. M. van, Bywater, R., Findlay, J. B., Hendlich, M., Hooft, R. W. & Vriend, G. (1996). *J. Comput.-Aided Mol. Des.* **10**, 255–262.

Appleby, T. C., Erion, M. D. & Ealick, S. E. (1999). *Structure Fold. Des.* **7**, 629–641.

Appleby, T. C., Mathews, I. I., Porcelli, M., Cacciapuoti, G. & Ealick, S. E. (2001). *J. Biol. Chem.* **276**, 39232–39242.

Ashour, O. M., Al Safarjalani, O. N., Naguib, F. N., Goudgaon, N. M., Schinazi, R. F. & el Kouni, M. H. (2000). *Cancer Chemother. Pharmacol.* **45**, 351–361.

Basso, L. A., Santos, D. S., Shi, W., Furneaux, R. H., Tyler, P. C., Schramm, V. L. & Blanchard, J. S. (2001). *Biochemistry*, **40**, 8196–8203.

Bennett, E. M., Anand, R., Allan, P. W., Hassan, A. E., Hong, J. S., Levasseur, D. N., McPherson, D. T., Parker, W. B., Secrist, J. A. III, Sorscher, E. J., Townes, T. M., Waud, W. R. & Ealick, S. E. (2003). *Chem. Biol.* **10**, 1173–1181.

Brünger, A. T., Adams, P. D., Clore, G. M., DeLano, W. L., Gros, P., Grosse-Kunstleve, R. W., Jiang, J.-S., Kuszewski, J., Nilges, M.,

Pannu, N. S., Read, R. J., Rice, L. M., Simonson, T. & Warren, G. L. (1998). *Acta Cryst.* D**54**, 905–921.
Burling, F. T., Kniewel, R., Buglino, J. A., Chadha, T., Beckwith, A. & Lima, C. D. (2003). *Acta Cryst.* D**59**, 73–76.
Caradoc-Davies, T. T., Cutfield, S. M., Lamont, I. L. & Cutfield, J. F. (2004). *J. Mol. Biol.* **337**, 337–354.
Cha, S. M. (1989). *Yonsei Med. J.* **30**, 315–326.
Drabikowska, A. K., Lissowska, L., Draminski, M., Zgit-Wroblewska, A. & Shugar, D. (1987). *Z. Naturforsch. C*, **42**, 288–296.
Drabikowska, A. K., Lissowska, L., Veres, Z. & Shugar, D. (1987). *Biochem. Pharmacol.* **36**, 4125–4128.
Ealick, S. E., Rule, S. A., Carter, D. C., Greenhough, T. J., Babu, Y. S., Cook, W. J., Habash, J., Helliwell, J. R., Stoeckler, J. D., Parks, R. E. Jr, Chen, S. & Bugg, C. E. (1990). *J. Biol. Chem.* **265**, 1812–1820.
Evans, G. B., Furneaux, R. H., Lewandowicz, A., Schramm, V. L. & Tyler, P. C. (2003). *J. Med. Chem.* **46**, 5271–5276.
Evans, G. B., Furneaux, R. H., Schramm, V. L., Singh, V. & Tyler, P. C. (2004). *J. Med. Chem.* **47**, 3275–3281.
Goudgaon, N. M., Naguib, F. N., el Kouni, M. H. & Schinazi, R. F. (1993). *J. Med. Chem.* **36**, 4250–4254.
Gouet, P., Courcelle, E., Stuart, D. I. & Metoz, F. (1999). *Bioinformatics*, **15**, 305–308.
Jones, T. A., Zou, J.-Y., Cowan, S. W. & Kjeldgaard, M. (1991). *Acta Cryst.* A**47**, 110–119.
Kicska, G. A., Long, L., Horig, H., Fairchild, C., Tyler, P. C., Furneaux, R. H., Schramm, V. L. & Kaufman, H. L. (2001). *Proc. Natl Acad. Sci. USA*, **98**, 4593–4598.
Koellner, G., Bzowska, A., Wielgus-Kutrowska, B., Luic, M., Steiner, T., Saenger, W. & Stepinski, J. (2002). *J. Mol. Biol.* **315**, 351–371.
Kouni, M. H. el, Goudgaon, N. M., Rafeeq, M., Al Safarjalani, O. N., Schinazi, R. F. & Naguib, F. N. (2000). *Biochem. Pharmacol.* **60**, 851–856.
Kouni, M. H. el, Naguib, F. N., Niedzwicki, J. G., Iltzsch, M. H. & Cha, S. (1988). *J. Biol. Chem.* **263**, 6081–6086.
Kouni, M. H. el, Naguib, F. N., Panzica, R. P., Otter, B. A., Chu, S. H., Gosselin, G., Chu, C. K., Schinazi, R. F., Shealy, Y. F., Goudgaon, N., Ozerov, A. A., Ueda, T. & Iltzsch, M. H. (1996). *Biochem. Pharmacol.* **51**, 1687–1700.
Kraulis, P. J. (1991). *J. Appl. Cryst.* **24**, 946–950.
Krenitsky, T. A., Barclay, M. & Jacquez, J. A. (1964). *J. Biol. Chem.* **239**, 805–812.
Laskowski, R. A., MacArthur, M. W., Moss, D. S. & Thornton, J. M. (1993). *J. Appl. Cryst.* **26**, 283–291.
Leer, J. C., Hammer-Jespersen, K. & Schwartz, M. (1977). *Eur. J. Biochem.* **75**, 217–224.
Levesque, D. L., Wang, E. C., Wei, D. C., Tzeng, C. C., Panzica, R. P., Naguib, F. N. M. & el Kouni, M. H. (1993). *J. Heterocycl. Chem.* **30**, 1399–1404.
Lewandowicz, A., Shi, W., Evans, G. B., Tyler, P. C., Furneaux, R. H., Basso, L. A., Santos, D. S., Almo, S. C. & Schramm, V. L. (2003). *Biochemistry*, **42**, 6057–6066.
Mao, C., Cook, W. J., Zhou, M., Federov, A. A., Almo, S. C. & Ealick, S. E. (1998). *Biochemistry*, **37**, 7135–7146.
Mao, C., Cook, W. J., Zhou, M., Koszalka, G. W., Krenitsky, T. A. & Ealick, S. E. (1997). *Structure*, **5**, 1373–1383.
Merritt, E. A. & Bacon, D. J. (1997). *Methods Enzymol.* **277**, 505–524.
Morgunova, E., Mikhailov, A. M., Popov, A. N., Blagova, E. V., Smirnova, E. A., Vainshtein, B. K., Mao, C., Armstrong, S. R., Ealick, S. E., Komissarov, A. A., Linkova, E. V., Burlakova, A. A., Mironov, A. S. & Debabov, V. G. (1995). *FEBS Lett.* **367**, 183–187.
Murshudov, G. N., Vagin, A. A., Lebedev, A., Wilson, K. S. & Dodson, E. J. (1999). *Acta Cryst.* D**55**, 247–255.
Naguib, F. N., el Kouni, M. H., Chu, S. H. & Cha, S. (1987). *Biochem. Pharmacol.* **36**, 2195–2201.
Naguib, F. N., Levesque, D. L., Wang, E. C., Panzica, R. P. & el Kouni, M. H. (1993). *Biochem. Pharmacol.* **46**, 1273–1283.
Niedzwicki, J. G., Chu, S. H., el Kouni, M. H., Rowe, E. C. & Cha, S. (1982). *Biochem. Pharmacol.* **31**, 1857–1861.
Niedzwicki, J. G., el Kouni, M. H., Chu, S. H. & Cha, S. (1981). *Biochem. Pharmacol.* **30**, 2097–2101.
Niedzwicki, J. G., el Kouni, M. H., Chu, S. H. & Cha, S. (1983). *Biochem. Pharmacol.* **32**, 399–415.
Orr, G. F., Musso, D. L., Kelley, J. L., Joyner, S. S., Davis, S. T. & Baccanari, D. P. (1997). *J. Med. Chem.* **40**, 1179–1185.
Otwinowski, Z. & Minor, W. (1997). *Methods Enzymol.* **276**, 307–326.
Park, K. S., el Kouni, M. H., Krenitsky, T. A., Chu, S. H. & Cha, S. (1986). *Biochem. Pharmacol.* **35**, 3853–3855.
Pugmire, M. J. & Ealick, S. E. (1998). *Structure*, **6**, 1467–1479.
Pugmire, M. J. & Ealick, S. E. (2002). *Biochem J.* **361**, 1–25.
Pugmire, M. J., Cook, W. J., Jasanoff, A., Walter, M. R. & Ealick, S. E. (1998). *J. Mol. Biol.* **281**, 285–299.
Schramm, V. L. (2002). *Biochim. Biophys. Acta*, **1587**, 107–117.
Schramm, V. L. (2003). *Nucleic Acids Res. Suppl.*, pp. 107–108.
Shi, W., Basso, L. A., Santos, D. S., Tyler, P. C., Furneaux, R. H., Blanchard, J. S., Almo, S. C. & Schramm, V. L. (2001). *Biochemistry*, **40**, 8204–8215.
Shi, W., Ting, L. M., Kicska, G. A., Lewandowicz, A., Tyler, P. C., Evans, G. B., Furneaux, R. H., Kim, K., Almo, S. C. & Schramm, V. L. (2004). *J. Biol. Chem.* **279**, 18103–18106.
Singh, V., Shi, W., Evans, G. B., Tyler, P. C., Furneaux, R. H., Almo, S. C. & Schramm, V. L. (2004). *Biochemistry*, **43**, 9–18.
Vita, A., Amici, A., Cacciamani, T., Lanciotti, M. & Magni, G. (1986). *Int. J. Biochem.* **18**, 431–435.
Walter, M. R., Cook, W. J., Cole, L. B., Short, S. A., Koszalka, G. W., Krenitsky, T. A. & Ealick, S. E. (1990). *J. Biol. Chem.* **265**, 14016–14022.
Zhang, Y., Cottet, S. E. & Ealick, S. E. (2004). *Structure*, **12**, 1383–1394.